Tearing as a test for mechanical characterization of thin adhesive films

EUGENIO HAMM[1], PEDRO REIS[2], MICHAEL LEBLANC[3], BENOIT ROMAN[4] AND ENRIQUE CERDA[1]*

[1]Departamento de Física and CIMAT, Universidad de Santiago, Av Ecuador 3493, Santiago, Chile
[2]Department of Mathematics, Massachusetts Institute of Technology, Cambridge, Massachusetts 02139, USA
[3]Department of Physics and JFI, University of Chicago, Chicago, Illinois 60637, USA
[4]PMMH, UMR 7636 CNRS/ESPCI/Paris6/Paris7, 10 rue Vauquelin, 75231 Paris cedex 5, France
*e-mail: ecerda@lauca.usach.cl

Published online: 30 March 2008; doi:10.1038/nmat2161

Thin adhesive films have become increasingly important in applications involving packaging, coating or for advertising. Once a film is adhered to a substrate, flaps can be detached by tearing and peeling, but they narrow and collapse in pointy shapes. Similar geometries are observed when peeling ultrathin films grown or deposited on a solid substrate, or skinning the natural protective cover of a ripe fruit. Here, we show that the detached flaps have perfect triangular shapes with a well-defined vertex angle; this is a signature of the conversion of bending energy into surface energy of fracture and adhesion. In particular, this triangular shape of the tear encodes the mechanical parameters related to these three forms of energy and could form the basis of a quantitative assay for the mechanical characterization of thin adhesive films, nanofilms deposited on substrates or fruit skin.

We have all had the experience of unsuccessfully trying to remove a rectangular strip from a roll of adhesive tape by scratching the edge with a fingernail. When pulling on the partially detached piece, the strip annoyingly narrows, detaches and the final tear is often too short to be useful. Similar difficulties are experienced when trying to remove wallpaper, a sticker or a package label adhered to a solid surface. Although the experience can make us feel incompetent, the runaway tear may in fact be taking a natural physical path. This behaviour is shared by many other adhesive films that are of great importance in a number of industrial applications, such as packaging (wrappers and sealing tapes), light reflectors or polarizers in coatings and adhering stickers as panels and labels in advertising. In general, these films must be resilient to deformation when used as physical barriers in packaging, but at the same time readily tearable by hand. In addition, their adhesive strength depends on the substrate. They must be weak enough when in contact with certain surfaces to allow the films to be stored (as in a roll of tape), but strong enough when put in contact with the desired substrate. All of these properties are involved in determining the geometrical shapes observed when a film is ripped apart. Here, we show how elasticity of thin sheets couples with adhesion and fracture to produce distinct shapes characterizing the tearing process.

We have carried out a combined experimental and theoretical study to explore this coupling of elasticity, adhesion and fracture, in a simplified geometry. A schematic diagram of our experiments is shown in Fig. 1a, inset and Fig. 2 (more details on the experiments are given in the Methods section). We adhere a thin elastic sheet to a solid flat surface and cut two notches on one of its edges such that a rectangular flap is created, which is then pulled at a constant speed. The two crack tips (located at the edge of the flap) are initially parallel, but as the flap starts being pulled they propagate both forwards and inwards as the material progressively de-adheres from the substrate. Eventually, the two tips converge to a point and the strip detaches completely, leaving behind a triangular tear. This thinning and finite-time break-up of the material is reminiscent of the self-similar pinch-off observed during liquid drop detachment[1]. The observed tears in adhesive films do not show strong signs of plastic deformation as opposed to the tears studied by Atkins[2–4] in metallic plates. This is not surprising because reversible deformations would help in the effective use and re-use of these films. Fortunately, this helps simplify the theoretical analysis that explains the narrowing of the tears.

Scanned profiles of three representative tears are shown in Fig. 1b in which only the width of the initial flap (distance from the initial two notches) was changed. The sides of the flap are straight and make the same angle θ with the axis of symmetry of the tear, independently of the size of the initial flap. Figure 1a shows a plot of the width of the tear, W, as a function of the distance to the detachment point, L, and shows that the shape follows the linear relation $W \sim L$ over almost three decades, ranging from tens of centimetres to a fraction of a millimetre. We note that a cutoff to this linear scaling occurs for length scales smaller than $L \sim 1$ mm. In the following, we focus mainly on the linear regime.

Following Griffith's theory of fracture[5], we propose a simple mechanism based on elasticity to understand our experimentally obtained tear shapes. A pulling force deforms the surface and focuses elastic energy in a ridge or fold that joins the flap with the film. This energy can be released in two ways: by decreasing its curvature (advancing the crack in the pulling direction) or by simply reducing the width of the ridge (the cracks move inwards). The actual direction is a combination of both effects, but always leads to a narrowing of the tear. Note that this situation differs from that of oscillatory tearing of thin films by a blunt object[6,7], where the fracture is driven by in-plane forces without mediation of a localized fold.

The total energy of the system that quantifies the above outlined mechanism is

$$U = U_E + 2\gamma ts + \tau A, \qquad (1)$$

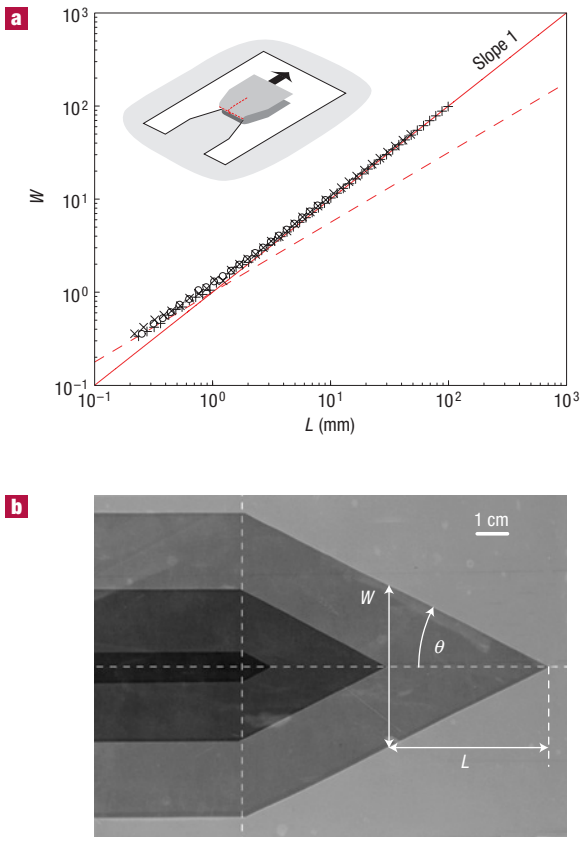

Figure 1 Three rectangular flaps of adhesive film were cut and pulled at the same speed, and the resulting tears were digitally scanned. a, Width versus length in millimetres on a log–log plot for the flaps with initial widths of 10 (open circles), 50 (times symbols) and 100 (plus symbols) mm. Solid red lines have been included for comparison. Inset: Schematic representation of the experimental set-up. The film is attached to a solid plane using an adhesive. Then a flap is cut and joined to a metal rod that acts as a winch drum. The rotation of the rod pulls the flap and starts the tearing. **b**, The tear shapes obtained in the experiment are shown overlapped. Here, L is defined as the distance from a given point along the axis of symmetry (horizontal dashed line) to the tip and is measured on a high-resolution scanned image of the tear. The width W is the distance between the two sides of the tear along the perpendicular line to the axis of symmetry.

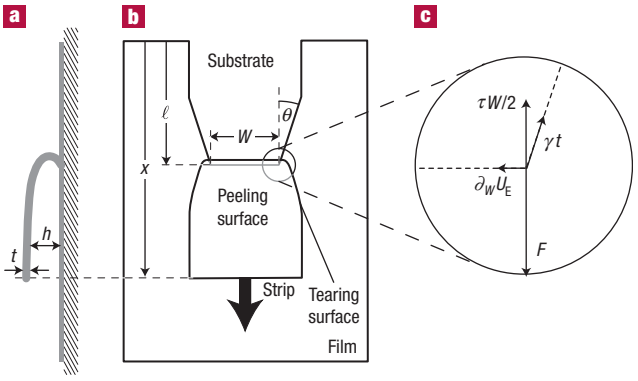

Figure 2 Schematic diagram showing the side and top views of the experiment and the geometrical parameters involved to describe the shape of the tear. **a**, Side view of the flap. The distance h gives the 'height' of the fold. **b**, Top view of the experiment. **c**, The close up shows a view of the tear at the position of the crack tip. The fracture propagation can be interpreted as the balance of four vectorial forces: two of them due to adhesion and fracture force, and the other two due to the pulling force and the inward force $\partial_W U_E$.

where the first, second and third terms are the elastic, fracture and adhesion energies, respectively. Here, t is the film thickness, s is the length of the crack, γ is the work of fracture of the film, τ is the adhesive energy required to peel a unit area of interface and A and $2ts$ are the peeling and tearing surface areas, respectively. The factor 2 in the fracture energy term accounts for the fact that two fracture paths are propagating along the film. In the following, because the work of fracture always comes in the combination γt and this parameter has a dimension of a force, we refer to γt as the 'fracture force'.

Assuming that the end of the flap is always at an angle of 180° from the reference plane defined by the solid wall, we conclude that the elastic energy is only a function of the tip displacement, x, and the length of the strip along its axis of symmetry, ℓ (Fig. 2b). The excess of length $2\ell - x$ is folded near the detachment line (Fig. 2a,b), so that we expect the elastic energy to be a function of the tip displacement in this combination. Thus, the energy as a function of the geometrical parameters must be of the form $U_E = U_E(2\ell - x, W)$.

The crack tip advances to a position that minimizes the total energy[5]. In a displacement-controlled experiment, the first variation of U with respect to the geometrical parameters is $\delta U = (\partial_W U_E)_{x,\ell}\delta W + (\partial_\ell U_E)_{x,W}\delta\ell + 2\gamma t\delta s + \tau W\delta\ell$. In addition, the force is given by the work theorem as $F = (\partial_x U_E)_{W,\ell}$ for a quasistatic fracture propagation. This equation combined with the specific dependence of the elastic energy on the geometrical parameters yields for the energy minimum, $\delta U/\delta s = 0$, the condition

$$0 = -2(\partial_W U_E)_{x,\ell}\sin\theta - 2F\cos\theta + 2\gamma t + \tau W\cos\theta, \qquad (2)$$

where $\sin\theta = -\delta W/2\delta s$ and $\cos\theta = \delta\ell/\delta s$. The constitutive relation for the force $F = F(x, \ell, W)$ allows the elimination of the parameter x in equation (2). Hence, an implicit relation between the force and the tearing angle of the form $F = F(\theta, \ell, W)$ is obtained. To find the fracture path, we require that the tear follows the direction where a minimal force is necessary for the advancement of the crack tips, that is $(\partial_\theta F)_{\ell,W} = 0$. An implicit derivative of equation (2) gives the equivalent condition $\partial_\theta(\delta U/\delta s) = 0$ that is usually referred to as the maximum-energy-release-rate criterion[5]. Thus, a second condition is obtained as

$$0 = -2(\partial_W U_E)_{x,\ell}\cos\theta + 2F\sin\theta - \tau W\sin\theta. \qquad (3)$$

Equations (2) and (3) have a clear interpretation in terms of static equilibrium of in-plane forces which is schematically represented in Fig. 2c. These forces, acting on one half of the strip, are: the fracture force γt resisting crack propagation, the operator pulling force F opposed to the adhesion energy dissipation $\tau W/2$ and the lateral elastic energy gradient $\partial_W U_E$. In this interpretation, it is clear that a convergent or divergent tear depends on the sign of $\partial_W U_E$. The forces projected along the forward and sidewise directions give the equivalent equations

$$F = \tau\frac{W}{2} + \gamma t\cos\theta \qquad (4)$$

$$(\partial_W U_E)_{x,\ell} = \gamma t\sin\theta. \qquad (5)$$

Equation (4) is very similar to the Young equation for the description at the solid–liquid–vapour contact point of a drop on a solid surface[8]. It is also the generalization of the equation obtained by Kendall[9], who studied the peeling of an adhesive film. Our description shows that the pulling force is balanced by two forces: that of adhesion of the film to the substrate and that of fracture. Moreover, it predicts that the force decreases proportionally to the flap width and has a finite value $\gamma t \cos\theta$ when the width tends to zero. This implies that near the tip, adhesion forces are negligible and the fracture force is the only remaining obstacle to detachment.

To experimentally check equations (4) and (5), we use three different films of thickness 50 μm (M50), 70 μm (M70) and 90 μm (M90). The films are very similar to scotch tape. In fact, film M70 is an adhesive film used as a window polarizer. The other two films were fixed to a solid wall by using adhesives. These three materials are brittle: they are easy to tear and on fracture leave behind two planar crack lips. Although the fracture force is different for each film, the adhesion energy is the parameter that can be more easily varied systematically. This can be done in two ways: (1) by pulling the flap at different speeds and (2) by using different substrates. The relation between adhesion energy and speed, $\tau = \tau(v)$, is not fully understood even though this dependence has been extensively studied in recent years[10]. It explains the interesting dynamics observed when peeling an adhesive tape such as stick–slip and chaos[11,12]. Here, we use low speeds where $\tau(v)$ is a monotonically increasing function[12]; however, the exact relation of adhesion on speed is not necessary in our analysis, because we directly measure the adhesion in each experiment.

Figure 3a shows the shape of the resulting tears when the film M70 is adhered to the same substrate and flaps are pulled at different speeds. By increasing the speed, the adhesion energy increases and the tears become shorter. This monotonic increase of the adhesion energy with speed can be confirmed in Fig. 3b,c. Here, the pulling force, F, as a function of the flap width, is plotted for a number of experiments at a variety of pulling speeds (using the M50 and M70 films). A linear decay of the force with the width of the tear is observed, as predicted by equation (4). Specifically, Fig. 3b, inset shows the measured force for the tears shown in Fig. 3a. As the values of the slope are smaller for M70 in Fig. 3b than for the same material in Fig. 3b, inset, we conclude that the adhesion energy is smaller for the first case. We can also observe that the straight lines that fit each set of data have approximately the same intercept with the y axis. This is in accordance with equation (4). The tear angles for all of the experiments have $\cos\theta \approx 1$, so that the intercept gives an estimation of the fracture force. A further check is obtained by repeating the experiments for M50. The fracture force is roughly proportional to the thickness; hence, we expect a lower value for the intercept. Figure 3c shows that this is indeed the case. Using the intercept in the force versus width graph after rescaling by the corresponding factor $\cos\theta$, we can make a better estimation of the fracture force for each material (see the Supplementary Information for details). The values $\gamma t = 1.5 \pm 0.1$ N and $\gamma t = 0.6 \pm 0.1$ N for the films M70 and M50, respectively, corresponding to the data shown in Fig. 3, and $\gamma t = 1.9 \pm 0.1$ N for the film M90, are the average results obtained from this method. In addition, the value of the fracture force obtained in this way is consistent with the direct measurement of the force needed to start a tear by pulling a rectangular flap when the film is not adhered to a substrate, but held on its boundaries. In this case, equation (4) is reduced to $F = \gamma t$. We use this configuration extensively for a first evaluation of the fracture force (this is a variation of the standard test ASTM D1938-06, see the Methods section).

We now turn to study equation (5), which unlike equation (4), is sensitive to the value of the tear angle θ. To use this equation, we need to obtain the exact expression for the elastic energy. In general, it can be a difficult task to compute precisely how the elastic energy is distributed in the strip because the typical displacements observed are of the order of the system size. In this situation, out-of-plane bending deformation is coupled to stretching, and the standard approach to quantify the elastic energy involves solving the highly nonlinear equations known as the Föppl–von Karman equations[13,14]. To avoid this approach, we take advantage of the film being strongly adhered to a substrate. This configuration helps to keep the lines across the flap width with zero curvature, allowing the surface to deform only along its longitudinal direction (see Fig. 2). Thus, the surface is isometric to a plane[15]. The deflection can therefore be analysed in terms of the classical elastica of Euler[14] that accounts for arbitrary planar deformations of a sheet, and the

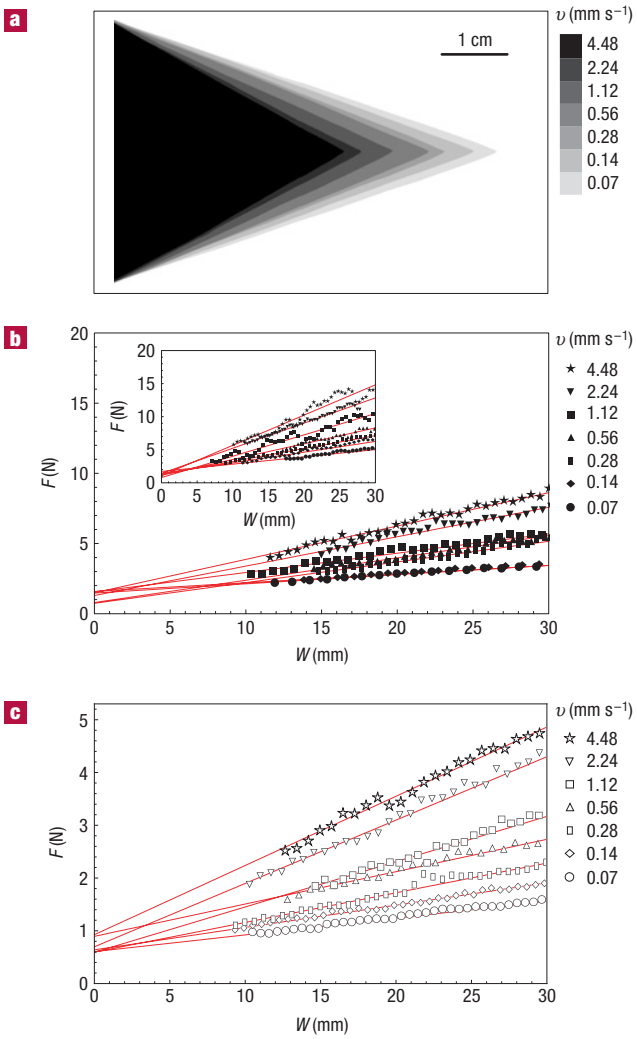

Figure 3 Force versus width for different materials and substrates. **a**, Experiments using M70. The film was adhered to a substrate and then a 4-cm-wide flap was pulled. The experiment was repeated seven times at the pulling speed shown in the legend. The seven resulting scanned tears are shown overlapped in the figure. **b**, The pulling force versus width for runs made at different speeds. Inset: The same experiments when the film M70 was adhered to a substrate with a stronger adhesive affinity, so that a larger force is necessary to detach the tear for a given pulling speed. Note that the intercept remains the same. **c**, Experiments using M50. A lower force is needed to detach the flap for an equivalent pulling speed and the intercept has a lower value.

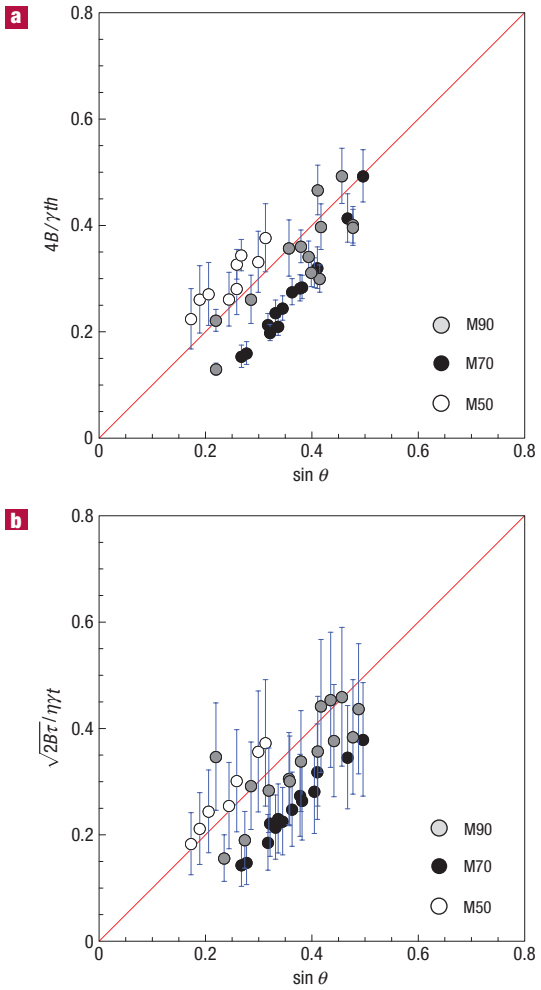

Figure 4 The angle of tearing for experiments with three different materials. In our experiments, we used M50 ($B=(3.0\pm0.1)\times10^{-5}$ N m, $\gamma t=0.6\pm0.1$ N), M70 ($B=(5.5\pm0.1)\times10^{-5}$ N m, $\gamma t=1.5\pm0.1$ N) and M90 ($B=(1.5\pm0.1)\times10^{-4}$ N m, $\gamma t=1.9\pm0.1$ N). **a**, The angle of tearing versus $4B/\gamma th$. The variation of the angle and average distance h is produced by changing the substrate and varying the pulling speed. The red line shows the theoretical prediction. The error bars show the uncertainty obtained from the estimated error of each parameter. **b**, The angle of tearing versus $(2B\tau)^{1/2}/\eta\gamma t$.

elastic energy available for fracture can be easily obtained. It yields $U_E=4BW/h$, where B is the bending stiffness and h is the distance of the flap from the solid wall (Fig. 2a). Equation (5) is now

$$\sin\theta=\frac{4B}{\gamma th}. \qquad (6)$$

Figure 4a shows that our experiments confirm this relation. Furthermore, because we find the tear angle to be constant in our experiments (triangular tear shapes), this relation implies that h is a constant, throughout the tearing process. This prediction can be confirmed in Fig. 5, inset where the distance h is shown for two tears made at different speeds for the same material. It can also be directly observed in the Supplementary Information video.

So far, we have shown that relations (4) and (5) are satisfied by our experiments. It remains to be explained why these equations imply that the fracture trajectories are straight lines. Relations (4) and (5) are a closed system of equations for the fracture trajectory because the force is given by the constitutive relation

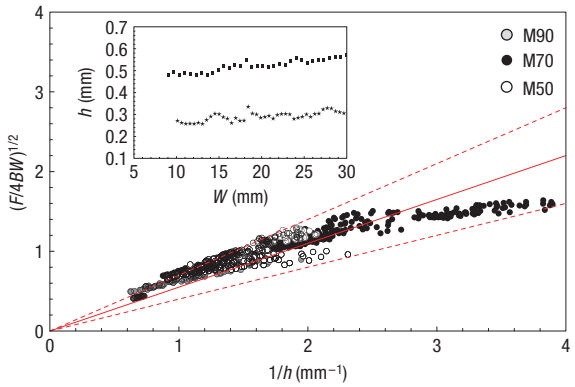

Figure 5 Value of the parameter η extracted from the experiments. The combination $(F/4BW)^{1/2}$ as a function of the inverse of the distance h (both in mm^{-1}). The experiments were carried out for M50, M70 and M90 by using the same speeds and substrates as the experiments in Fig. 3. The straight solid line with a slope $\eta\approx0.55$ is the best fit for all of the experimental points and the dashed lines show the error bounds of our estimate (see the Methods section for details). The inset gives the distance h as a function of width W for two representative experiments with M70 adhered to the same substrate, but at the speeds $v=0.28\ \mathrm{mm\,s^{-1}}$ (rectangles) and $v=4.48\ \mathrm{mm\,s^{-1}}$ (stars). The distance h is approximately a constant for each experimental run. Thus, the variation in the distance h in the main figure is obtained from using different substrates and pulling speeds.

$F=(\partial_x U_E)_{W,\ell}=4\eta^2BW/h^2$ where $\eta^2=-\partial_x h$. This relation is consistent with the force measurements shown in Fig. 5, but with a lower value of η than the value $\eta=1$ expected for a perfectly elastic strip (see the Methods section for details). Equation (4) is now

$$4\eta^2\frac{BW}{h^2}=\tau\frac{W}{2}+\gamma t\cos\theta. \qquad (7)$$

Assuming that η is a constant parameter, equations (6) and (7) can be combined into a first-order differential equation for $W(\ell)$ that determines the fracture trajectory. Instead of solving this equation, we observe that for large values of W, the last term in equation (7) is negligible. Hence, the distance h must have the constant value $h=2\eta(2B/\tau)^{1/2}$. It shows that a larger pulling speed increases the adhesion energy, makes the fold joining the crack tips smaller (h decreases, see Fig. 5, inset), and, following equation (6), the tears shorter. This relation in equation (6) yields

$$\sin\theta=\frac{(2B\tau)^{1/2}}{\eta\gamma t}. \qquad (8)$$

Thus, the trajectories are straight lines with a tear angle determined by three material constants. With the value of the parameter $\eta=0.55\pm0.15$ extracted from Fig. 5 and the measured values of the material constants B, τ and γt, we plot all of our data in Fig. 4b using equation (8). Note that the larger error bars of Fig. 4b compared with the ones in Fig. 4a are due mainly to our conservative estimate for the error of η (for details, see the Methods section). We finally comment that equation (8) is no longer valid when the flap width is so small that adhesion energy is comparable to the fracture force. The conditions for this to happen are given in the Supplementary Information.

We close by pointing out that the formalism we have developed can be used to investigate the mechanical properties of thin adhesive films. As thickness is reduced owing to new technologies, traditional methods used to measure mechanical properties of a material in bulk form are not applicable. For instance, a simple uniaxial test applied to a specimen to study its elastic and fracture

properties leads to unexpected mechanical behaviour such as stress localization[16] and wrinkling[17]. This same new behaviour has recently motivated the development of new techniques for the measurement of the elastic properties of thin films[18,19]. Similarly, our results suggest that the coupling between elasticity, adhesion and fracture, imprinted in a tear shape, can be used to evaluate mechanical properties of thin films. The angle observed is a combination of three parameters: the elastic stiffness of the film, its fracture force and the adhesion energy with the substrate. Thus, the measurement of the tear angle gives a method to obtain one parameter when the other two are already known. Take a simple example: a typical adhesive tape designed for sealing (3M-305) has a width $W = 4.8\,\mathrm{cm}$ and a bending stiffness that can be easily measured as $B \approx 2.7 \times 10^{-6}\,\mathrm{N\,m}$. The force needed to start a tear when a rectangular flap is pulled with a dynamometer and the tape is not in contact with a substrate is $\gamma t \approx 2 \times 10^{-1}\,\mathrm{N}$. We can now predict the adhesion energy when the tape is applied to different substrates by using the formula $\tau = (\eta\gamma\sin\theta)^2/2B$. For instance, when the tape is adhered to a metal panel and pulled at a constant speed of $5\,\mathrm{mm\,s^{-1}}$, the tear angle is $\theta \approx 16°$. Combining all of these measurements yields $\tau \approx 1.7 \times 10^{2}\,\mathrm{N\,m^{-1}}$. This estimate can be directly compared with the value of the adhesion energy provided by the manufacturer which is $\tau \approx 2.2 \times 10^{2}\,\mathrm{N\,m^{-1}}$ (this is given by the standard test ASTM D-3330, see the Methods section). Our analysis can help to evaluate the mechanical properties of more complex systems that behave similarly to adhesive films. It is a common observation that some fruits, such as peaches, plums or tomatoes, produce triangular tears when peeled. Our set-up enables measurement of the fracture force and adhesive energy of the fruit skin. However, the skin has a natural curvature that makes it difficult to measure bending stiffness with our methods. We show in the Supplementary Information how our formula gives an estimate of the bending stiffness for tomato fruits consistent with reported values[20].

METHODS

GENERAL

The polymer films we used in the experiments are M70: commercial adhesive film (Sun-Gard Frost Matte 100), thickness 70 μm; M50 and M90: bi-oriented polypropylene film (BOPP, Innovia), 50 μm and 90 μm thick. The film was adhered to a glass plate and a parallel flap 4 cm wide and of variable length was then cut and detached starting from the edge of the film. In the case of M50 and M90, we uniformly fixed the films to a glass plate by using adhesives (3M double-sided tape). The strip was then pulled with the help of a PC-driven stepper motor and a transmission system that leads to uniform pulling in all runs of the experiment, at speeds ranging from a few $\mathrm{mm\,s^{-1}}$ down to $10^{-2}\,\mathrm{mm\,s^{-1}}$. To avoid anisotropic effects, we cut and pulled flaps in the film always in the same direction. Pulling force F was measured by attaching the strip to a force sensor (SCAIME type K25).

FOLD SIZE MEASUREMENT

To measure the distance h, we projected a laser sheet of thickness 0.5 mm (WorldStar) over the strip at an angle close to 30°. Images were taken vertically above the reference plane of the film enabling us to measure the deflection of the laser line. This deflection gives, after calibration, the value of h. In addition, from the same image, we determined the width of the strip, W, at each position of the tearing process (see the Supplementary Information, video).

BENDING STIFFNESS MEASUREMENT

The value of the bending stiffness B of the materials used in the experiments was obtained by the following method. A sheet of material $26 \times 3\,\mathrm{cm}$ was immobilized at a sharp table edge and the distance of the material from the wall at the lower boundary, where curvature is zero, was measured. This distance enables us to obtain the bending stiffness of the material[13]. The experiment was repeated four times for different strips of the same material. The bending stiffness was obtained as the mean value of the four measurements and its uncertainty was estimated as one standard deviation of the mean. To avoid possible anisotropies in bending stiffness, we measured this parameter in the same direction as the direction of bending in our experiments.

ANALYSIS OF PARAMETER η

The size of the fold h is exactly the excess of length $h = 2\ell - x$ for a cylindrical deformation; hence, $\eta = 1$. A lower value of η observed in the experiments implies that the fold shows more rigidity than predicted by elasticity. Two effects could explain this lack of response to the pulling force. First, plasticity could make the sheet more rigid near the fold, so that a saturation value for the value of h could be reached. Second, the adhesive behaves in a more complex way than the simple model used in equation (1) and long interaction effects due to adhesive filaments could also modify the shape of the fold.

To obtain the effective value of η, we use all of our data for M50, M70 and M90 (Fig. 5) and find the best fit. It gives $\eta \approx 0.55$. However, there are small variations in the value of the parameter η when the fit is made with data for only one type of film. A safe assumption is that η lies between the maximum and minimum possible slopes obtained from the statistical analysis of our data. In Fig. 5, the probability is 68% that a measurement will fall inside the two dashed lines. This is approximately equivalent to the more graphical method[21] of plotting the straight lines with maximum and minimum slope that contains all of the data.

ASTM STANDARDS

Our evaluation of the fracture energy is a variation of the standard test method ASTM D1938-06 that measures the force necessary to propagate a tear by using a single crack. In this case, force and fracture force are connected by the equation $F = \gamma t/2$.

The method used by 3M to measure adhesion of pressure-sensitive tapes is defined by the ASTM standard D-3330. The tape is adhered to a stainless-steel panel and peeled from the panel at 180° at the specified rate $5.0 \pm 0.2\,\mathrm{mm\,s^{-1}}$. At the same time, the force required to peel the tape is recorded to obtain the adhesion. Note that these specifications are similar to the conditions used in our experiments.

Received 30 November 2007; accepted 27 February 2008; published 30 March 2008.

References

1. Eggers, J. Nonlinear dynamics and breakup of free-surface flows. *Rev. Mod. Phys.* **69**, 865–930 (1997).
2. Atkins, A. G. *Proc. 10th Congr. on Material Testing* 595–600 (Scientific Society of Mech. Engineers, Budapest, 1991).
3. Atkins, A. G. Opposite paths in the tearing of sheet materials. *Endeavour* **18**, 2–10 (1994).
4. Atkins, A. G. Ripping yarns. Science & public affairs. *Autumn* 19–23 (1994).
5. Lawn, B. *Fracture of Brittle Solids* 2nd edn (Cambridge Univ. Press, Cambridge, 2004).
6. Audoly, B., Reis, P. & Roman, B. Cracks in thin sheets: When geometry rules the fracture path. *Phys. Rev. Lett.* **95**, 025502 (2005).
7. Ghatak, A. & Mahadevan, L. Crack street: the cycloidal wake of a cylinder tearing through a thin sheet. *Phys. Rev. Lett.* **91**, 215507 (2003).
8. De Gennes, P. G., Brochard, F. & Quérés, D. *Capillarity and Wetting Phenomena* (Springer, New York, 2003).
9. Kendall, K. Thin-films: the elastic term. *J. Phys. D* **8**, 1449–1452 (1975).
10. Cortet, P. P., Ciccotti, M. & Vanel, L. Imaging the stick-slip peeling of an adhesive tape under a constant load. *J. Stat. Mech.* P03005 (2007).
11. Hong, D. C. & Yue, S. Deterministic chaos in failure dynamics: Dynamics of peeling of adhesive tape. *Phys. Rev. Lett.* **74**, 254–257 (1995).
12. De, R., Maybhate, A. & Ananthakrishna, G. Dynamics of stick-slip in peeling of an adhesive tape. *Phys. Rev. E* **70**, 046223 (2004).
13. Landau, L. & Lifshitz, E. M. *Theory of Elasticity* 3rd edn (Pergamon, New York, 1986).
14. Love, E. H. *A Treatise on the Mathematical Theory of Elasticity* (Dover, New York, 1944).
15. Struik, D. J. *Lectures on Classical Differential Geometry* (Dover, New York, 1988).
16. Witten, T. A. Stress focusing in elastic sheets. *Rev. Mod. Phys.* **79**, 643–675 (2007).
17. Cerda, E. & Mahadevan, L. Geometry and physics of wrinkling. *Phys. Rev. Lett.* **90**, 074302 (2003).
18. Stafford, C. *et al.* A buckling-based metrology for measuring the elastic moduli of polymeric thin films. *Nature Mater.* **3**, 545–550 (2004).
19. Huang, J. *et al.* Capillary wrinkling of floating thin polymer films. *Science* **317**, 650–653 (2007).
20. Matas, A. *et al.* Biomechanics and anatomy of *Lycopersicon esculentum* fruit peels and enzyme-treated samples. *Am. J. Bot.* **91**, 352–360 (2004).
21. Boisclair, G. & Pagé, J. *Guide des Sciences Expérimentales* 3rd edn (ERPI, Québec, 2004).

Acknowledgements

We thank the Chicago–Chile Material Collaboration Project (DMR-0303072), Ecos-Conicyt project No. C03E04 and are grateful for the help of Francisco Melo in whose laboratory this experiment was carried out. This article was also greatly improved by comments from M. Adda-Bedia, B. Audoly, A. Boudaoud, F. Melo and K. Niklas. E.H. and E.C. acknowledge FONDAP Grant No. 11980002 for financial support. E.C. acknowledges the support of Anillo ACT 15, Fondecyt Project No. 1050083 and thanks Mauricio Cerda for help with the computer software. B.R. acknowledges support from the French ministry of research—ACI 'structures minces', and PMR from the European funding MechPlant.

Correspondence and requests for materials should be addressed to E.C.

Supplementary Information accompanies this paper on www.nature.com/naturematerials.